Electromagnetic Interference Shielding Effectiveness of Graphite-Filled Polypropylene and Poly(ether imide) Based Composites

Pravin Sawai, Susanta Banerjee

Materials Science Centre, Indian Institute of Technology, Kharagpur 721302, India

Received 12 September 2007; accepted 25 January 2008
DOI 10.1002/app.28246
Published online 6 May 2008 in Wiley InterScience (www.interscience.wiley.com).

ABSTRACT: The electromagnetic interference shielding characteristics of polypropylene (PP) and poly(ether imide) (PEI) filled with synthetic graphite composites were studied. The thermal properties were characterized by differential scanning calorimetry and thermogravimetric analysis, whereas the morphologies of the composites were studied by scanning electron microscopy. The viscosity measurements were studied by advance rheometry. The measurements of shielding effectiveness (SE) were carried out in the frequency range 8–12 GHz (X-band range). The return loss and loss due to absorption were also measured as a function of frequency in the X-band range. It was observed that the SE of the composites was frequency dependent, and it increased with increasing frequency. The SE also increased with increasing filler loading. The PEI-based composites showed a higher SE compared to that of the PP-based composites. The correlation between SE and the conductivity of the various composites is also discussed. © 2008 Wiley Periodicals, Inc. J Appl Polym Sci 109: 2054–2063, 2008

Key words: composites; polyimines; structure–property relations; thermal properties

INTRODUCTION

With the rapid growth of electrical and electronics devices, which emit electromagnetic energy in the same frequency bands used by other users in markets, it becomes essential to limit and shield electronic equipment against all sources of interference[1] due to all of these electromagnetic energies. Electromagnetic interference (EMI) is basically electrical in nature and is due to unwanted electromagnetic emissions being either radiated or conducted. Metal is considered to be the best material for electromagnetic shielding, but it is expensive and heavy. On the other hand, the use of polymers for housing electronic devices is popular because they are lightweight, flexible, and less expensive. However, polymers are electrically insulating and transparent to electromagnetic radiation; that is, their inherent EMI shielding effectiveness (SE) is practically zero. To shield against EMI, the technical approach, which has been considered extensively, is to incorporate electrically conductive fillers in polymer matrices.[2] Various materials are selected for use in different microelectronic devices depending on their SE over different frequency ranges. They are also used in microwave applications to avoid interference due to unwanted electromagnetic waves. Thus, a number of researchers have endeavored to prepare electrically conductive composites as effective electromagnetic shielding materials;[3–15] however, both the conductivity and EMI SE have reported to be improved by the incorporation of electrically conductive fillers, including carbon black, graphite fibers, metal fibers, and metal particulates.[9,16] Various studies have been carried out on conductive plastics composites as EMI shielding materials.[13,16,17] Baker et al.[1] evaluated the SE of steel-fiber-filled acrylonitrile–butadiene–styrene rubber. Even carbon and glass fibers can be coated with metals, such as aluminum or nickel, to improve the SE of the composites; nickel-coated mica-filled low-density polyethylene can also be used as an effective shielding material.[18] Fibrous fillers, which are less expensive, are considered to be superior to other conductive fillers, such as powdery particles or flakes.[17] When polyacrylonitrile-based carbon fibers are compounded into the polymer matrix, they can improve not only the conductivity but also the strength of the composites.[2,19] The SE of poly(ether imide) (PEI) composites filled with conductive graphite and polypropylene (PP) based composites was investigated. In fact, this kind of conductive composite may also be used for applications such as typical antenna systems, anechoic chambers to prevent interference due to unwanted electromagnetic fields during measurement, radar cross sections, computer housing, PCB shielding, different types of pressure-sensitive switches, connector gaskets, and floor-heating elements. This article reports the results of the EMI SE and return loss (RL) of different com-

Correspondence to: S. Banerjee (susanta@matsc.iitkgp.ernet.in).

posites based on PEI and PP filled with conductive graphite over the X-band frequency range 8–12 GHz.

The aim of this study was to asses the EMI SE of polymer–graphite composites in the X-band frequency region and to compare the performance of these polymers. PEI was chosen in this study because it belongs to the polyimide family of polymers and has been proven to have the proper combination of mechanical properties, thermooxidative stability, and processability desirable in aerospace applications.[20] Moreover, it exhibits a much wider processing window than other polymers, which are interactable with high melting temperatures (T_m's) and viscosity and less solubility.[21–23] It can be easily processed with conventional extrusion and injection- or blow-molding machines. The cost of PEI-based composites may be slightly higher than that of PP-based composites. However, the difference is not significant because an adequate SE can be obtained for PEI-based composites at a relatively lower loading. In fact, the cost of these composites are cheaper than those of the metal or metal-filled systems.

EXPERIMENTAL

Materials

The orthodichlorobenzene and methanol used were from E. Merck (Mumbai, India); 4,4′-isopropylidenediphenoxy)bis(phthalic anhydride) (97%) and 1,3-phenylenediamine (99%) were purchased from Aldrich (Bangalore, India). The polymeric matrices used for the preparation of the composites were PEI and PP. PP (REPOL B250EG) was obtained from Reliance Industries, Ltd. (Hazira, India). Synthetic graphite powder was supplied by Graphite India, Ltd. (Bangalore, India; carbon = 98.5%, sulfur = 0.1%, iron = 0.4%, volatile matter = 0.5%, ash content = 0.5%, and particle size = 2–10 μm) and was used as a filler.

Preparation of PEI

PEI was prepared by the reaction of equimolar amounts of 4,4′-(4,4′-isopropylidenediphenoxy)-bis(phthalic anhydride) and 1,3-phenylenediamine in orthodichlorobenzene. A standard protocol of the solution polymerization technique was adopted, as reported elsewhere.[24] The number-average molecular weight of the synthesized PEI was 26,000, the polydispersity index was 2.6, and the glass transition of the synthesized PEI was 217°C.

Composite processing: Formulation of the mixes

Before processing, the PEI powder and PP pellets were dried *in vacuo* at 110°C for at least 24 h. The graphite powder was dried in a vacuum oven at 100°C for at least 12 h. The formulation of the polymer mixes containing graphite are given in Table I. The mixing of different composites was accomplished in a Brabender plasticorder PL2200 (mixer N50) equipped with two counterrotating rotors at 200°C for PP and 320°C for PEI, and mixing was carried out for a short time to prevent the effect of processing on the electrical conductivity and, thereby, EMI SE. The procedure was as follows: first, the polymer was melted, and then, graphite was incorporated into the molten polymer matrix. The mixed materials were taken out of the mixing chamber. The formulation are given in Table I. The mixes were compression-molded under a pressure of about 20 MPa at 320°C for poly(ether imide)/graphite (PEI/G) and 200°C for polypropylene/graphite (PP/G) composites for 10 min. The samples were allowed to cool to room temperature under the same pressure at a rate of 2°C/min.

TABLE I
Formulation of the PP/G and PEI/G Composites

Sample composition	Graphite (wt %)	PP (wt %)	PEI (wt %)
100/0	0	100	100
90/10	10	90	90
80/20	20	80	80
70/30	30	70	70
60/40	40	60	60
50/50	50	50	50
40/60	60	40	40

CHARACTERIZATION

Electrical conductivity and EMI shielding measurements

The volume resistivity (ohm cm) of composites was measured on a compression-molded square slab (length = 1 cm, thickness = 1.6 mm, and breadth = 1 cm). A Keithley (Keithley Instrument, Inc., Cleveland, OH) 230 programmable voltage source text fixture was used to measure volume resistance. This equipment allowed resistivity measurement up to 10^{18}. The pressed samples were put into the four-point conductivity apparatus, a constant current (I) was applied to the sample through two outside probes with the help of a direct-current power source, the steady voltage across the other inside two probes (V) was determined,[25] and with the following equations. the resistivity (R; ohm cm) was calculated:

$$R = V/I \tag{1}$$

$$\rho = \Omega wt/L \tag{2}$$

where Ω is the resistance, ρ is the resistivity, w is the width of sample, t is the thickness of sample, and L is the length between inner probes.

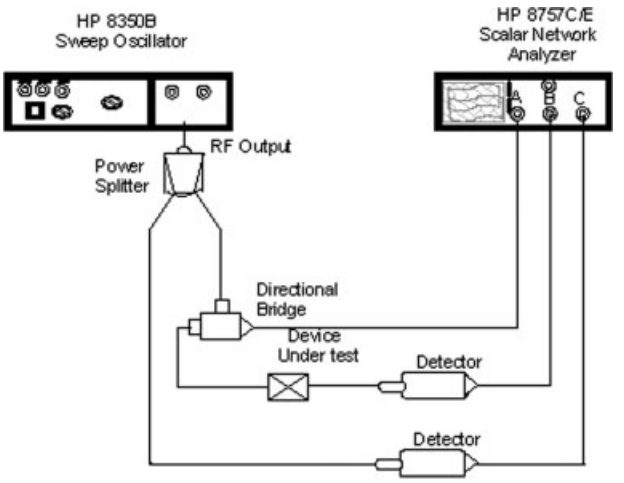

Figure 1 Schematic diagram of a basic scalar coaxial system for the measurement of transmission loss and RL. RF, radio frequency.

The measuring setup used for the EMI SE is schematically shown in Figure 1. The setup consisted of a sweep oscillator (model HP 8350B, Hewlett Packard, USA), a power splitter, a detector, and a scalar network analyzer (model HP 8753 C/E, Hewlett Packard). All of these instruments were connected to a test chamber. The sample holder in the test chamber was changed according to the measurement frequency range. The SE was measured with the coaxial cable line method. SE in the frequency range 8–12 GHz was measured with an X-band wave guide as sample holder. Samples with thicknesses of 4.96 mm were used during measurement. We carried out the EMI shielding measurement for each sample by continuously sweeping the frequency over ranges of 8–12 GHz. When SE was found to be greater than 40 dB, some noise was encountered during measurement; otherwise, the result obtained was a smooth curve of SE against frequency as obtained from the instrument.

Differential scanning calorimetry (DSC)

The melting and crystallization behaviors of the PP and the glass-transition temperature (T_g) of PEI were measured with a Netzsch DSC 200 PC model instrument (Netzsch, Germany). Polymer samples weighing about 10 mg closed in aluminum pans were used throughout the experiment. Indium of high purity was used to calibrate the DSC temperature and enthalpy scales. The samples (10 mg) of the PP-based composites were heated from room temperature to 200°C and cooled to room temperature at a rate of 20°C/min under a nitrogen atmosphere, and the PEI-based composites were heated from room temperature to 300°C at a rate of 20°C/min under a nitrogen atmosphere.

Thermogravimetric analysis (TGA)

The decomposition process of the composites was studied with a Netzsch TG 209 f1 thermogravimetric analyzer in nitrogen from 50 to 800°C at a heating rate of 10°C/min.

Advance rheometry

Samples of disk-shaped specimens with a thickness of 2 mm and a diameter of 25 mm were prepared. An AR 1000 rotational rheometer (TA Instruments, New Castle, DE) was used to measure the viscosities. The measurement of the dynamic viscosities was performed with a parallel plate fixture (diameter = 25) with a gap distance of 1.2 mm; the strain was kept at 10% to ensure linear viscoelasticity. and the temperature used was 200°C for PP-based composites and 300°C for PEI-based composites. This study was conducted under air to prevent degradation.

Scanning electron microscopy

Scanning electron microscopy analysis was done with a Jeol (Japan) JSM-5800 scanning electron microscope. This was done to observe the morphology of the failure surfaces of the composites and the dispersion of graphite in the composites. Samples were fractured in liquid nitrogen, and the fractured surfaces were gold-plated and then mounted over an aluminum stub with double-sided electric adhesive tape. The vacuum was on the order of 10^{-4} to 10^{-6} mmHg during the scanning of the composite samples.

Tensile testing

The tensile tests were carried out with a Tinius Olsen (Horsham, PA) materials testing system (model H50KS) at room temperature with a gauge length of 25 mm and a crosshead speed of 1.25 mm/min.

RESULTS AND DISCUSSION

Basic theory of EMI shielding

An electromagnetic shielding material is a material that attenuates radiated electromagnetic energy. Electromagnetic radiation can be divided into near-field and far-field regions. In the near field, the electromagnetic signal can be predominantly an electric vector or a magnetic vector, depending on the nature of the source. In the far field, plane waves exist, in which the electric and magnetic vectors have an equal ratio in phase and are orthogonal to each other. We are most concerned with the plane radiation (far field) in measuring SE. EMI is defined as spurious voltage and current induced in the electronics circuit by external sources. SE is a number

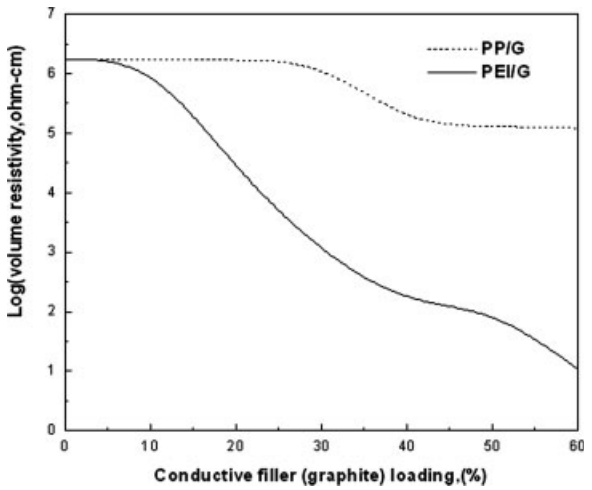

Figure 2 Volume resistivity against the conductive filler for the PP-and PEI-based composites.

that quantifies the amount of attenuation typical of a particular material.[26] If P_{inc} is the incident power density at a measuring point before the shield is in place, P_{trans} is the transmitted power density at same measuring point after the shield is in place, and P_{ref} is the reflected power density at same measuring point

$$SE = 10\log(P_{trans}/P_{inc}) \tag{3}$$

$$RL = 10\log(P_{ref}/P_{inc}) \tag{4}$$

It is evident that, for a lossless material

$$P_{inc} = (P_{ref}/P_{trans}) \tag{5}$$

where P_{abs} can be quantified as the absorbed power inside the dielectric and

$$P_{abs} = 1 - P_{ref}/P_{inc} - P_{trans}/P_{inc} \tag{6}$$

where P_{abs} is the power absorbed of a lossy dielectric.[27] However, EMI is the consequence of reflection loss, transmission or absorption loss, and internal reflection loss at exiting interfaces of the incident electromagnetic waves in the sample. These three losses are interrelated by[28]

$$S = (R + A + B)(\text{dB}) \tag{7}$$

where S is the shielding effectiveness or insertion loss, which represents the reduction (dB) of the level of an electromagnetic field at a point in space after a conductive barrier is inserted between that point and the source. R is the sum of the initial reflection losses (dB) from both surfaces of the shield exclusive of additional reflection losses, A is the absorption or penetration loss (dB) within the barrier itself, and B is the internal reflection loss at exiting interface (dB). This term may be either positive or negative and is negligible for $A \geq 15$ dB.

For plane wave radiation, R and A may also be calculated from[29]

$$R = 108 + \log(G/\mu f) \tag{8}$$

$$A = 1.32t[G\mu f]^{1/2} \tag{9}$$

where G is the conductivity of the sample relative to copper, μ is the magnetic permeability of the sample relative to a vacuum or copper ($\mu = 1$), f is the frequency of radiation (MHz), and t is the thickness of the sample (cm). It is observed from these equations that reflection loss is directly proportional to the log of conductivity and inversely proportional to the permeability of the sample and also to the log frequency of the incident electromagnetic wave. How-

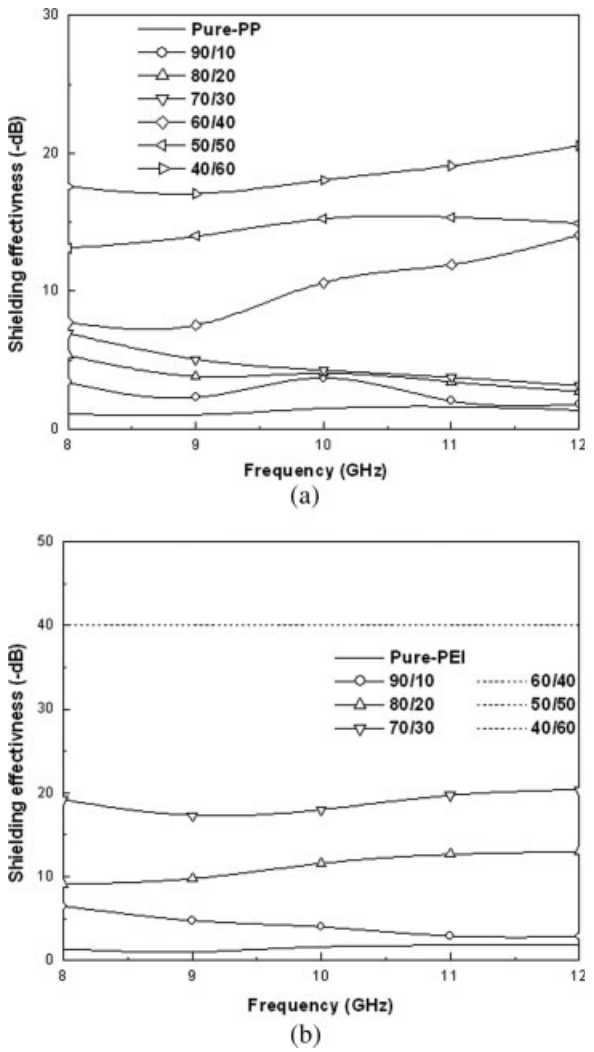

Figure 3 Variation of SE over the X-band frequency range (8–12 GHz) of the (a) PP-based composites containing different weight percentages of PP/G and (b) PEI-based composites containing different weight percentages of PEI/G.

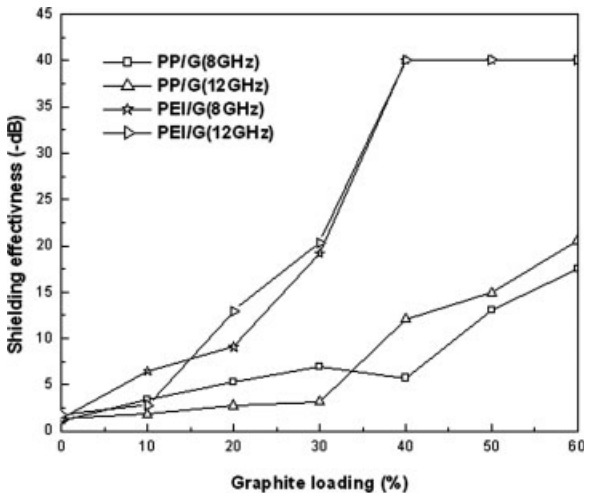

Figure 4 SE at 8 and 12 GHz as a function of filler loading for PP- and PEI-based composites.

ever, absorption loss is directly proportional to the thickness of the sample and the square root of frequency, conductivity, and permeability of the sample.

EMI, SE, RL, and absorption loss (AL) measurements

The electrical resistivity of PP- and PEI (graphite)-based composites are represented in Figure 2. The resistivity decreased with increasing conductive graphite loading. The PEI-based composites showed much higher conductivity than the PP-based ones. However, the percolation limit for conduction was higher for the PEI-based composites compared to the PP-based ones.

The SE values of different composites containing graphite over the frequency range 8–12 GHz (X-band region) are presented in Figure 3. The following results were observed

1. The SE of the composites increased with filler loading at all frequencies of incident radiation.
2. The SE of all of the composites appreciably increased when the frequency was changed from a lower to a higher frequency domain; for example, the composite PEI/G (70/30) containing 70 wt % PEI and 30 wt % graphite exhibited a shielding level between 19.16 and 20.36 dB over 8–12 GHz, respectively.
3. An amorphous-polymer-based composite was more effective than the crystalline polymer in providing high EMI shielding.

Figure 4 shows the variation of SE with graphite loading at fixed frequencies of 8 and 12 GHz, respectively. Interestingly, with increasing graphite loading, SE increased, but the rate was much faster for the PEI-based composites to for the PP-based composites. The SE of the 60 wt % graphite loading in PP was 17.58–20.54 dB over the frequency range

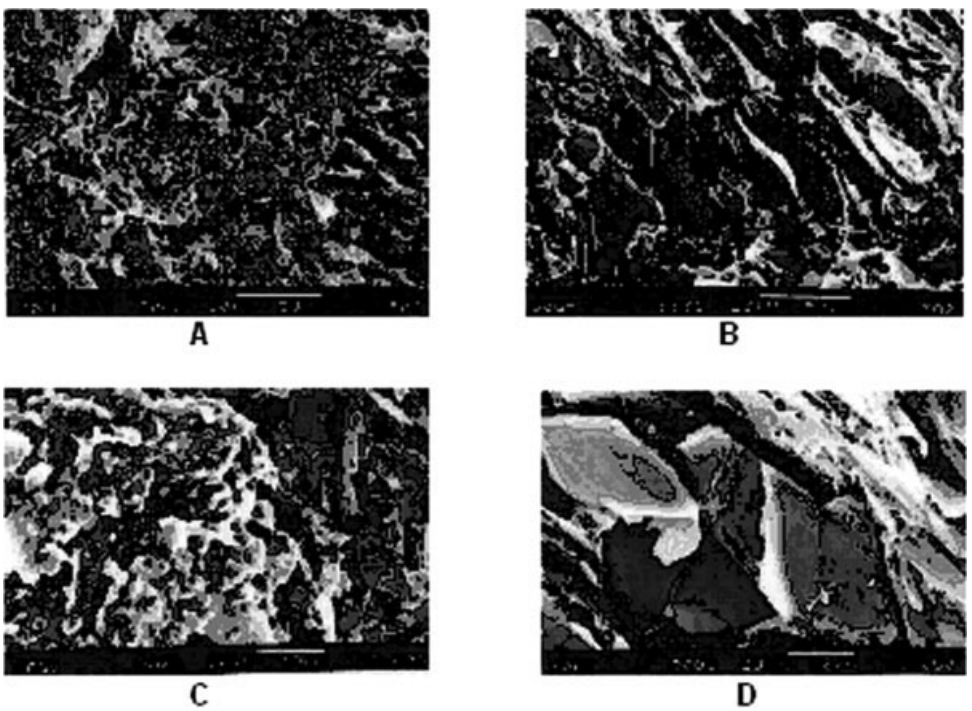

Figure 5 Scanning electron micrograph of 60 wt % graphite loaded in the PEI and PP composites at (A,B) 500 and (C,D) 2000×.

8–12 GHz, but this SE value was achieved in only 30 wt % graphite loading in PEI (19.16–20.36 dB). The SE of 40 wt % graphite loading in the PEI-based composite was 40 dB, and the SE at 50 and 60 wt % graphite loading had an average value of 40 dB. This was because the graphite concentration assumed almost a saturated limit around 40 wt % of the PEI-based composite. The change in conductivity remained marginal up to the critical concentrations. Then, the increase in conductivity was abrupt; that is, the insulation polymer matrix became conductive and above the critical concentration because of the formation of conductive networks. However, above this critical concentration, the change in conductivity with the graphite loading was only marginal; hence, this loading would be the optimum choice for effective shielding from these composites. The network formed due to distribution of the conducting filler inside the PEI matrices behaved like a conducting mesh, which intercepted electromagnetic radiation. The size of the mesh generally determines the effectiveness of shielding. The finer the mesh size is, the better is the SE. However, the size of the mesh is also related to the frequency of the incident radiation that will be intercepted. The SE depends on the thickness of the material, its electrical characteristics. and the nature of the incident radiation.[30] Increasing the specimen thickness would increase the amount of graphite intercepting the incident wave and make the network openings smaller. This orientation of the conducting filler inside this composite produced openings, which affected the coupling of the electromagnetic wave. If the openings were electrically small, the coupling was mainly due to the tangential magnetic field and the electric field component normal to the specimen plane. The higher SE of the PEI-based composites compared to those of the PP-based ones at the filler loading was due to the higher conductivity of the PEI-based composites than those of PP-based ones. The conductive particle aggregation led to the formation of continuous conductive networks in the insulating PP matrix. Graphite particles already have aggregating tendencies, which may be of two types, known as primary and secondary structures. Some of these aggregates (secondary structure) easily break down during mixing, whereas the primary structure is relatively permanent and difficult to break. Even the primary structure may undergo some partial breakdown because of strong shearing action during mixing. The magnitude of the shearing action intensifies if the matrix to which graphite is added is tough, that is, if the matrix has a high viscosity. Extensive structure breakdown has a retarding effect on the formation of continuous conductive networks through particle aggregation. The PEI-based composites exhibited higher conductivities and higher SE compared to the PP-based

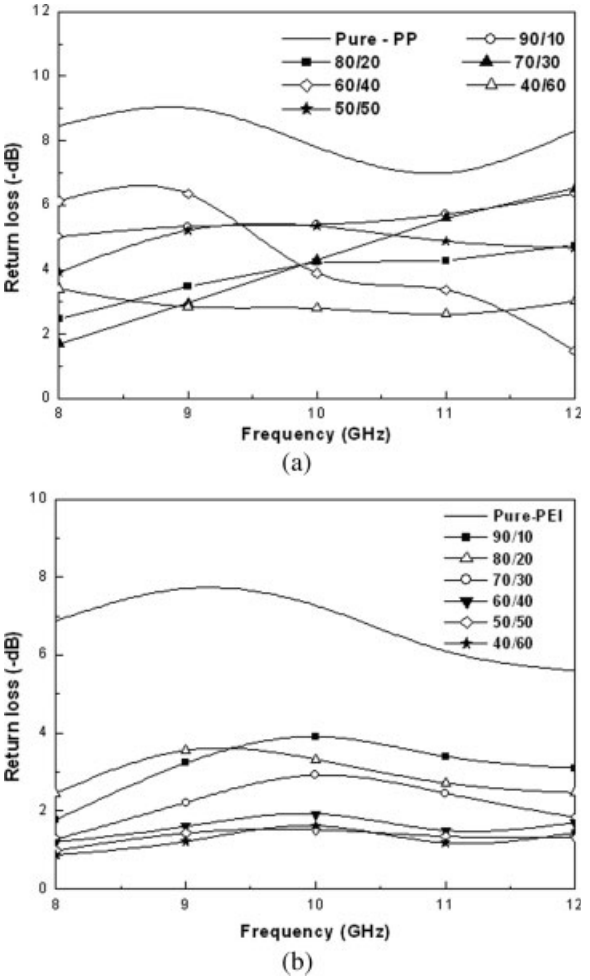

Figure 6 (a) Variation of RL versus frequency in the X-band frequency range (8–12 GHz) of the (b) PP-based composites containing different weight percentages of PP/G and (b) PEI-based composites containing different weight percentages of PEI/G.

ones; PEI, being a softer matrix compared to PP, caused a lesser degree of breakage during mixing. The network formation in graphite-filled composites was observed from scanning electron micrographs (Fig. 5).

A reversed trend is observed in RL versus frequency at different weight percentages of graphite loading, as shown in Figure 6. This shows that composites with a higher value of SE had a lower value of RL. For example, the PEI-based composites with 40 wt % graphite loading had an SE of 40 dB, whereas the RL of this composite was 1.7 dB at 12 GHz. Also, the result of the RL measurements shows that RL was frequency dependent. The uneven variation of RL against frequency was due to the random distribution of the conducting graphite inside the specimen, which led to the formation of voids of different sizes in the conducting mesh. These voids also affected RL because of their effect on the external reflection. In addition, RL and absorption loss made

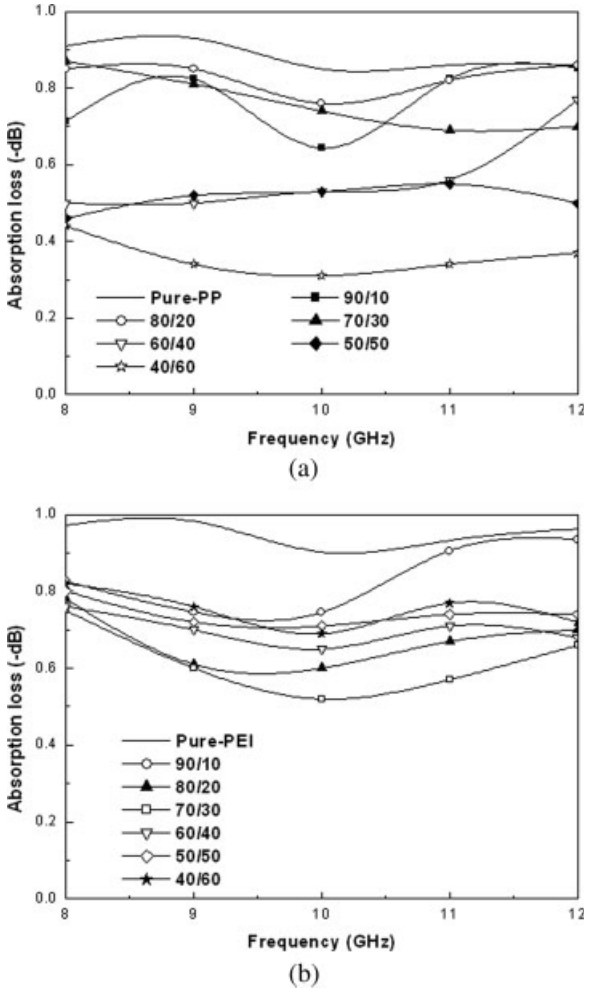

Figure 7 Plot of absorption loss versus frequency over the X-band region (8–12 GHz) for the (a) PP-based composites containing different weight percentages of PP/G and (b) PEI-based composites containing different weight percentages of PEI/G.

significant contributions to total SE. The change in absorption loss for the PP and PEI composites filled with graphite with frequency is shown in Figure 7. It is well established that the SE of a conductive composite is related to its conductivity. The SE depends not only on the conductivity but also on the reflection and absorption coefficient of the dispersed filler and its size, shape, and distribution in the matrix.[18] The void space between the filler aggregates depends on the distribution of filler in the matrix. The SE and RL also depend on the polymer viscosity, its polarity and the aspect ratio, structure, and size of the particulate filler and their distribution in the matrix. The maximum SE was found for PEI-based composites having a 40 wt % graphite loading. The voids in the conductive composite affected the absorption loss and RL due to their effects on the internal reflection, as discussed earlier. The most interesting feature of these conductive graphite-filled PEI-based composites was that the shielding was much more effective than that of the PP-based composites. For example, the PEI-based composites at 40 wt % graphite loading had an SE of 40 dB. A higher loading of graphite was also attempted to understand the loading effect in better way and to see whether the SE could be enhanced. However, at more than 40 wt % graphite loading in PEI, there was no significant enhancement in SE. Loadings of graphite more than 40 wt % induced the mixing problem and also decreased the mechanical properties to a great extent. PP at 60 wt % graphite loading had an SE value of 20.5 dB at 12 GHz.

Thermal properties (DSC and TGA)

DSC analysis

Figure (8) shows the DSC thermograms. The PP-based composites were obtained at a scan rate of 20°C/min. Here, the main purpose of this technique

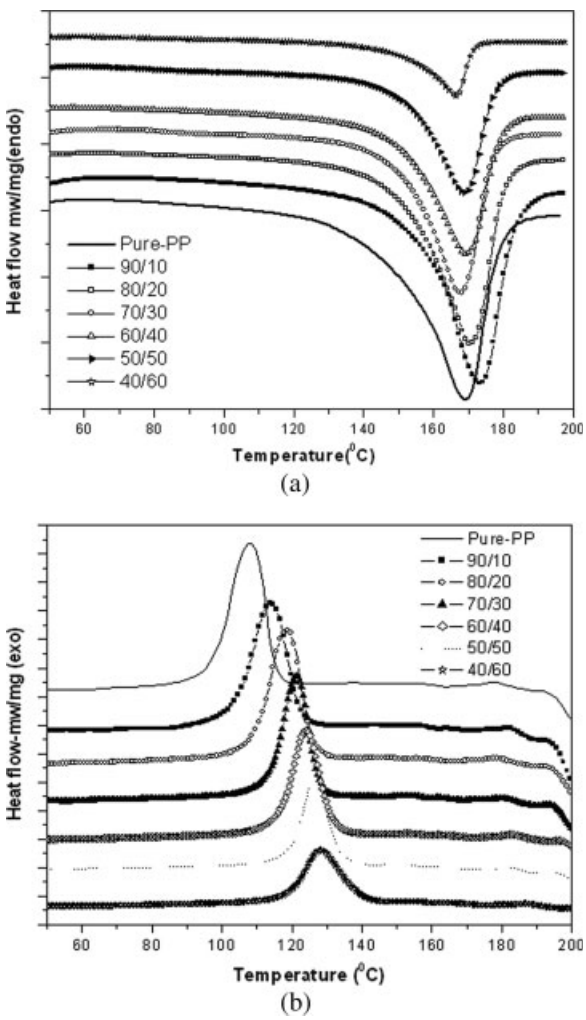

Figure 8 DSC spectra of the (a) PP/G (T_m), (b) PP/G (T_c).

TABLE II
Thermal Properties for the Composites (from DSC)

	PP/G composites					PEI/G composites	
Sample composition	T_m (°C)	ΔH_m (J/g)	T_c (°C)	ΔH_c (J/g)	Crystallinity (%)	T_g (°C)	ΔC_P (J g^{-1} K^{-1})[a]
100/0	169	69.89	108.1	83.27	39.84	217.9	0.259
90/10	173.3	56.71	113.9	69.81	30.17	213.4	0.189
80/20	170.3	54.8	118.7	64.19	28.12	210.7	0.153
70/30	167.8	43.81	121.3	50.80	24.34	213.8	0.149
60/40	169.3	42.34	124.0	45.17	20.14	213.3	0.132
50/50	168.9	32.6	126.4	34.04	17.23	215.3	0.106
40/60	166.4	22.56	128.5	27.45	13.96	215.3	0.110

[a] Change in the specific heat.

was to show the effect of melting, crystallinity, and rate of crystallization. With the incorporation of graphite, the melting peaks were shifted to the right side compared to the pure PP, and the change in enthalpy also decreased. This was due to the increasing graphite weight percentage, which acted to reduce the mobility of the polymer chain segments. The crystallization temperature (T_c) increased almost linearly with increasing filler quantity, and the crystallinity decreased. This was consistent with a change in the mechanism of crystallization associated with the addition of graphite (e.g., a change from homogeneous to heterogeneous nucleation).[31]

In the PEI-based composites, T_g and the change in the specific heat decreased as the weight percentage of the graphite increased and the polymer weight percentage decreased. This indicated that the mobility of the polymer chains was reduced because of the constraint effect of graphite.[32] T_m, enthalpy at melting (ΔH_m), T_c, enthalpy at crystallization (ΔH_c), degree of crystallinity (%), T_g, and change in specific heat of the PP- and PEI-based composites are tabulated in Table II. The SE was lower for the PP-based composite because of the crystallization behavior compared to the amorphous PEI-based composites.

TGA

TGA of the PP-based composites was carried out from 50 to 650°C under nitrogen at rate of 10°C/min. Figure 9(a) shows that the TGA curve of PP/G composites exhibited mass loss steps and the maximum degradation temperature. The thermal stability of the PP-based composites was evident up to 340°C. A weight loss was observed from 340 to 480°C. The degradation temperature, mass change (%) from 340 to 480°C, and residual mass (%) at 650°C of the samples are tabulated in Table III.

TGA of the PEI/G composites was carried out from 50 to 800°C under nitrogen at a rate of 10°C/min. Figure 9(b) shows that the TGA curve of PEI/G composites exhibited mass loss steps and the maximum degradation temperature. Thermal stability of the PEI-based composites was evident up to 465°C. A weight loss was observed from 465 to 800°C. Degradation temperature, mass change (%) from 465 to 800°C, and residual mass (%) at 800°C of the samples are tabulated in Table III.

The PEI-based composites were more stable than the PP-based composites. Weight loss (%) decreased

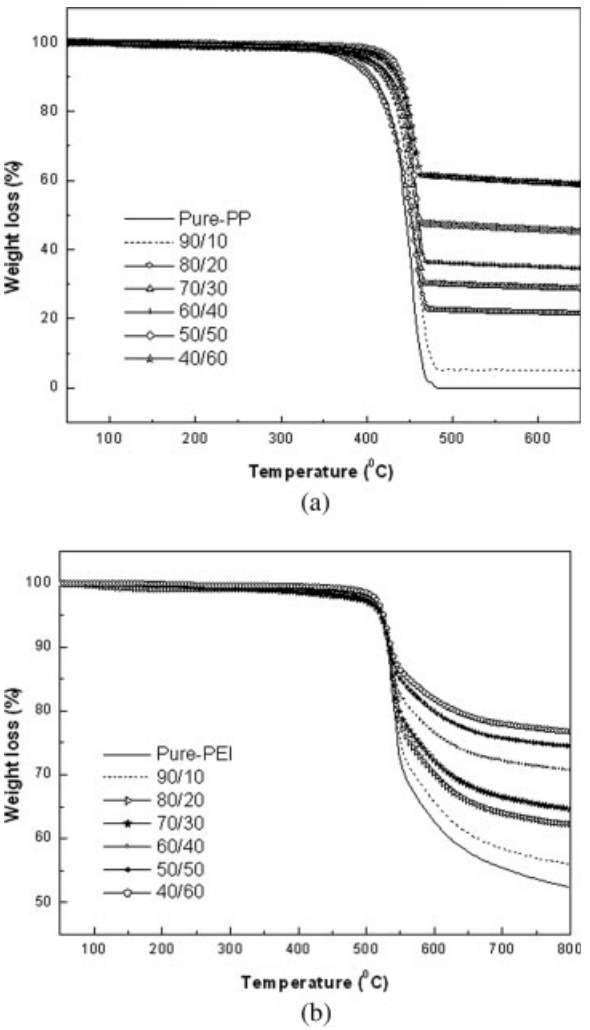

Figure 9 Thermal spectra thermogravimetry curve for the (a) PP/G and (b) PEI/G composites with different weight percentage ratios.

TABLE III
Thermal Properties of the Composites (from TGA)

Sample composition	PP/G composites			PEI/G composites		
	Degradation temperature (°C)	Mass change (%)[a]	Residual mass (%)[b]	Degradation temperature (°C)	Mass change (%)[c]	Residual mass (%)[d]
100/0	453.5	99.18	00.13	539.6	46.04	52.39
90/10	458.3	89.19	10.91	540.0	43.60	54.73
80/20	457.4	75.44	21.29	539.0	37.11	61.43
70/30	458.2	68.20	28.52	537.7	34.42	63.63
60/40	458.4	61.06	34.36	534.0	28.84	70.12
50/50	456.7	51.42	48.52	532.8	25.25	73.92
40/60	458.0	37.04	58.53	532.4	23.27	76.23

[a] Mass change (%) from 340 to 480°C.
[b] Residual mass (%) at 650°C.
[c] Mass change (%) from 465 to 800°C.
[d] Residual mass (%) at 800°C.

and residual mass (%) increased with decreasing weight percentage of the polymer and increasing weight percentage of graphite in the composites.

Advance rheometry

An advance rheometer was used to determine the viscosities of both the PEI- and PP-based composites at 300 and 200°C. Figure 10 indicates that the viscosity of the PEI-based composites was higher that of than the PP-based composites. The viscosity increased quite sharply with increasing shear rate. The viscosity also increases with increasing weight percentage of graphite loading. However, the percolation limit for conduction was higher for the PEI-based composites than for the PP-based ones. This can be explained by the higher viscosity of the base PEI matrix compared to that of PP.

Mechanical properties of the conducting composites

The tensile strengths of the PP and PEI composites with different loading levels of graphite are tabulated in Table IV. As shown, the tensile strength of the PP-based composites decreased with the increasing graphite ratio in PP. This was because of the crystallinity effect of the PP. The tensile strength of the PEI/G composites progressively decreased with increasing graphite ratio in PEI. An experiment revealed that the maximum loading beyond the equimolar ratio of PEI and PP brought about the breakdown of the composite.[33] The tensile strength of the PEI-based composites was higher than that of the PP-based composites.

CONCLUSIONS

1. Between two polymeric systems, PEI and PP, the PEI-based composites were found to be more effective in providing EMI shielding when graphite was used as the conductive filler. Furthermore, the PEI-based composites exhibited

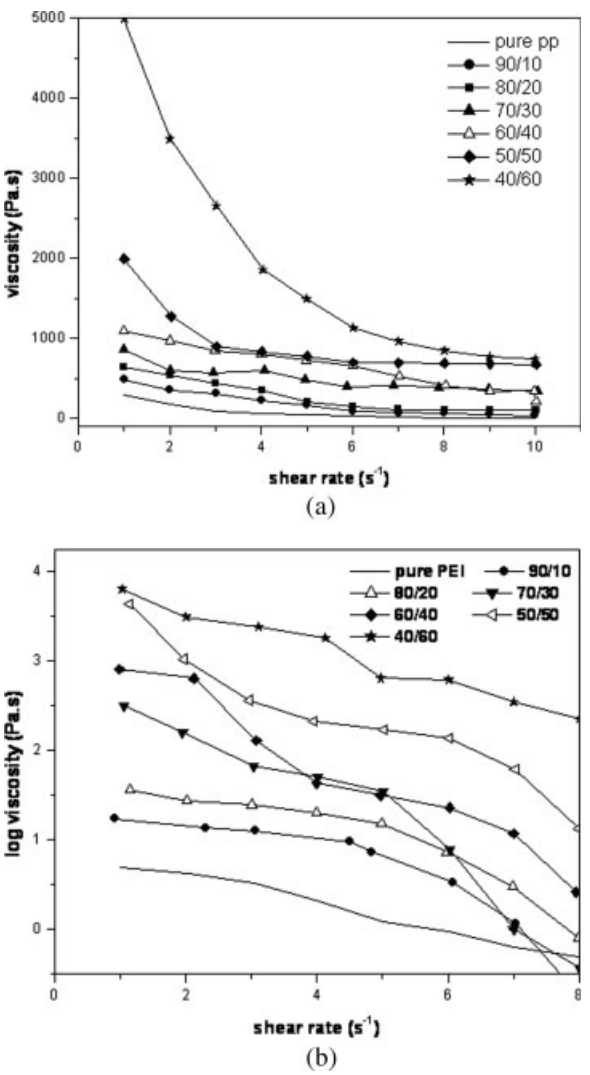

Figure 10 Flow properties of the (a) PP/G and (b) PEI/G composites with different weight percentage ratios.

TABLE IV
Mechanical Properties of the Composites

Sample composition	Tensile strength (MPa) of the PEI/G composites	Tensile strength (MPa) of the PP/G composites
100/0	71	21
90/10	46	20
80/20	32	18
70/30	21	15
60/40	15	15
50/50	10	11
40/60	3	10

higher SEs at lower filler loadings compared to the PP-based ones in the X-band frequency range, that is, 8–12 GHz.
2. The thermal stability and tensile strength of the PEI-based composites were higher than those of the PP-based composites.
3. The composites containing graphite were technically useful materials (SE ≥ 20 dB) in the X-band region.

The authors thank A. Chakraborty and Vishwanath Roy of the Department of Electronics and Electrical Communication Engineering, Indian Institute of Technology, Kharagpur, for their help and cooperation during the experimental work.

References

1. Baker, Z. Q.; Abelazeez, M. K.; Zihlif, A. M. J. Mater Sci 1988, 23, 2995.
2. Chiang, W.-Y.; Cheng, K.-Y. Polym Compos 1997, 18, 748.
3. Simon, R. M. Polym-Plast Technol Eng 1981, 17, 1.
4. Bigg, D. M. Polym Eng Sci 1977, 17, 842.
5. Maeda, O.; Yamakiand, J.; Katayama Y. Kobunshi Ronbunshu 1975, 32, 42.
6. Miyasaka, K.; Qatanabe, K.; Smithers, E.; Aida, H.; Sumita, M.; Lahikawa, K. Mater Sci 1982, 17, 1610.
7. Sumita, M.; Kijima, E.; Aida, H.; Miyasaka, K.; Ishikawa, K. Kobunshi Ronbunshu 1983, 40, 203.
8. Mukhopdhyay, R.; De, S. K.; Basu, S. Appl Polym Sci 1976, 20, 2575.
9. Bigg, D. M. Polym Eng Sci 1979, 19, 1188.
10. Kwan, S. H.; Shin, F. G. Tsui, W. L. J Mater Sci 1980, 15, 2978.
11. Nakagawa, T.; Suziki, K.; Koyama, H. Metal 1980, 50, 5.
12. Nakagawa, T.; Koyama, H.; Yanagisawa, A.; Suziki, K. Polym Prepr Jpn 1983, 32, 3033.
13. Sircar, A. K.; Wells, J. L. Polym Eng Sci 1981, 21, 809.
14. Bull, D. A.; Jackson, G. A.; Smithers, B. W. Radio Electron Eng 1981, 5, 505.
15. Oons, R. Pro Sci Eng Compos 1982, 2, 1029.
16. Jana, P. B.; Mallick, A. K.; De, S. K. Composites 1991, 22, 1.
17. Oshwa, Z.; Kobayashi, J. R. J Mater Sci 1987, 22, 4381.
18. Kortschot, M. T.; Woodhams, R. T. Polym Compos 1985, 6, 296.
19. Inconductive Polymers and Plastics; Wright, W. M.; Woodham, G. W.; Margolis, J. M., Eds.; Chapman & Hall: New York, 1989.
20. Wilson, D.; Stenzenberger, H. D.; Hergenrother, P. M. Polyimides; Chapman & Hall: London, 1990.
21. Yano, K.; Usuki, A.; Okada, A.; Kurauchi, T.; Kamigaito, O. J Polym Sci Part A: Polym Chem 1993, 31, 1942.
22. Yano, K.; Usuki, A.; Okada, A. J Polym Sci Part A: Polym Chem 1997, 35, 2289.
23. Tyan, H. L.; Liu, Y. C.; Wei, K. H. Chem Mater 1999, 11, 1942.
24. Ghosh, A.; Banerjee, S. J Appl Polym Sci 2008, 107, 1831.
25. Mironov, V. S.; Kim, J. K.; Park, M.; Lim, S.; Cho, W. K. Polym Test 2007, 26, 547.
26. White, X.; Donald, R. J.; Mardiguian, M. Electromagnetic Compatibility Handbook; Don White Consultants: Germany, 1973; Vol. 3.
27. Altam, D. Microwave Circuits; Van Nostrand: Princeton, NJ, 1964.
28. Reinaldo Perez, X. Handbook of Electromagnetic Compatibility; Academic Press, San Diego, California; 1995.
29. Duff, W. G. Fundamental of Electromagnetic Compatibility; Interference Control Tech.: Virginia; 1988; Vol. 1.
30. Wilson, P. F.; Adams, J. W.; Ma, M. T. Proc IEEE 1986, 74, 112.
31. Causin, V.; Marega, C.; Marigo, A.; Ferrara, G.; Ferraro, A. Eur Polym J 2006, 42, 3153.
32. Liu, T.; Tong, Y.; Zhang, W.-D. Compos Sci Technol 2007, 67, 406.
33. Koul, S.; Chandra, R.; Dhawn, S. K. Polymer 2000, 41, 9305.